On the formation of regular vegetation patterns

An experimental approach

Master's Thesis

by

Paul Berghuis

Utrecht University

May, 2021

Utrecht

Paul M.J. Berghuis (5726670)
p.m.j.berghuis@students.uu.nl
Utrecht University
45 ECTS

Supervisor: Dr. Angeles Garcia Mayor
Second reader: Dr. Jerry van Dijk
Sustainable Development -
Ecosystems and Environmental Change

Cover image: Photo of the experimental setup, with the different drought treatment becoming visible in the plots of *P.vaginatum* (March 2021).

Summary

An extensive field of research has been developed around the phenomenon of regular vegetation patterns in drylands. However, due to the large spatiotemporal scale of the studied systems, empirical evidence from manipulative experiments is missing. Proposed to produce regular vegetation patterns on a fine spatiotemporal scale, the grass *P.vaginatum* offers the opportunity to address this knowledge gap. This master thesis presents a first attempt on recreating fine scale regular vegetation patterns in an experimental setup. It was hypothesized, that similar to large scale dryland systems, a scale dependent feedback would apply for *P.vaginatum* and form regular patterns as reaction to drought stress. In the environmental homogenous conditions of a controlled lab setup the grass was being subjected to three different drought treatments for 45 days. During the experiment the spatial and temporal dynamics of the grass were monitored and measured. Despite a successful experiment, and in contrast to the hypothesis, for all drought treatments no regular pattern formation was observed. However, a substantial degree of spatial heterogeneity was captured for green cover as well as canopy temperature. The two most severe drought treatments (12.5% ET and 25%ET) showed transitional spatial aggregation, clustering in patches of green cover before stabilizing in a uniform dormant state. The wettest treatment (50%ET), showed a more constant spatial aggregation in green cover, but stabilization could not be confirmed. Compared to green cover, the heterogeneity in canopy temperature showed a higher degree of spatial aggregation and was more constant over time for all treatments. Following from the results of the experiment, the alternative cause of chill damage was highlighted for the field observed regular patterns of *P.vaginatum*. Moreover, recommendations for translating dryland modelling to fine scale regular vegetation patterns were given, stressing the importance of including case specific mechanisms. This study forms a starting point for future work aiming to provide the missing experimental evidence for regular vegetation patterns in drylands.

Preface

One year ago I started looking for a master thesis subject. At first I wanted to go on field work, but due to the pandemic, possible projects were uncertain and quickly enough became impossible. During the summer I came across a proposal for a so called 'high risk, high reward' project. Being familiar with the topic, vegetation patterns, I was quickly convinced this could be an exciting opportunity for my master thesis. Starting in September, after a few weeks I realized what the high reward entailed. Recreating regular vegetation patterns in a lab setup, that would be quite something, Building a suitable lab setup to make this possible grabbed all my attention. Stimulated by the enthusiasm of my supervisor and the people which became related to the project along the way, this lab setup became reality at the end of 2020. It was also at this point that the 'high risk' started to play a role. Since this was a first attempt, there was little reference for the choices we needed to make and no certainty of any success. In fact, a lot of things could go wrong. Luckily, they did not and a successful experiment followed. Although from a scientific point of view this master thesis may not have resulted in the intended 'high reward', on a personal level it certainly did, providing me an extremely learnful experience.

Paul Berghuis, Utrecht, 16th of May 2021

Contents

List of Tables

List of Figures

Introduction

Dryland ecosystems cover up to 45% of the world's land surface and inhabit more than 2 billion people, 90% of this area is located in developing countries (MEA, 2005; Prăvălie, 2016). Drylands are characterized by low and variable rainfall, often combined with limited soil nutrient availability, creating an ecosystem susceptible for external pressure. Problems in drylands are accumulating, as land cover change, population growth and climate change are believed to increase already existing water shortages (Huang et al., 2016; MEA, 2005; Reynolds, 2007). An important process making drylands such a critical area is extensive land degradation. This degradation is the result of a combination of human and climatic pressures. An estimated 10-20% of all drylands suffer from a form of degradation and biophysical feedbacks strongly limit recovery (D'Odorico, 2013; D'Odorico et al., 2019; Reynolds, 2007). Despite the large extent and impact of dryland degradation, quantitative data and predictive capacity is still very limited. Accurate quantification of dryland degradation is considered to be of the highest priority (Bestelmeyer et al., 2015; MEA, 2005).

One component which makes dryland degradation difficult to measure and predict is its nonlinear response to external pressure. Where external pressure can be slow and gradual, dryland ecosystems may react abruptly, resulting in sudden change or even a system transition (Scheffer et al., 2001; Scheffer et al., 2015). Due to the often harsh and extreme conditions, dryland vegetation is sparse. Organized in a patchy manner where water availability is insufficient to support a full homogenous cover. In these systems, so-called vegetation patterns can be recognized (Deblauwe et al.,2008). Vegetation patterns are an example of spatial self-organization, forming regular patterns present in a large variety of systems (for ecosystems see: Rietkerk & Van de Koppel, 2008). In drylands, regular patterns are thought to be the result of a scale dependent feedback referred to as the resource concentration mechanism (Aguiar and Sala 1999; Kefi et al., 2007; Lejeune, Couteron & Lefever, 1999; Rietkerk et al., 2002). The resource concentration mechanism consists of two components. First a short range positive feedback where higher plant density of a vegetated patch enables more surface water to infiltrate into the soil (this because of e.g. root penetration, the attraction of soil organisms, Puigdefábregas, (2005)). Second a long range negative feedback in the vicinity of the vegetation patch, where surrounding (bare) soil is less able to infiltrate surface water into the soil (because of e.g. crust forming, Eldridge, Zaady & Shachak, 2000). The lower infiltration capacity of bare soil leads to evaporation and runoff losses. In patchy drylands, vegetation increases infiltration beneath their own cover and moreover concentrates water by harvesting runoff from bare surroundings (Mayor et al., 2019). Using this resource concentration mechanism, vegetation can survive

increasing drought by self-organizing in an adapting pattern, typically transforming with increasing drought from gaps with bare ground, to a labyrinth of vegetation and bare soil, to spots of vegetation in a bare soil matrix (Barbier et al., 2006).

The development of spatial self-organization of vegetation in drylands is shown to exhibit non-linear behaviour (Kefi et al., 2010). Patchy drylands can have multiple stable states for similar environmental conditions (Bastiaanse et al., 2018). Two typical alternative stable states consist of a vegetated non-degraded state and an alternative bare degraded state. A dryland system in a stable vegetated state, is resistant to small perturbations (Mayor et al., 2013). However, when disturbance (e.g. overgrazing, drought) becomes too large, a threshold can be reached beyond which the system shifts to the degraded stable state. Such a sudden transition is referred to as a 'catastrophic shift' (Rietkerk & van de Koppel 1997; Scheffer et al., 2001; Schneider & Kéfi, 2016). Because of the existence of two stable states under the same environmental conditions (e.g., bi-stability), when the disturbance causing the catastrophic shift is removed, the system will not spontaneously return back to the former state. This so called hysteresis phenomena locks the system in the degraded state (Rietkerk et al., 2002; Saco et al., 2018). The multi-stability and nonlinearity of drylands makes it difficult to predict and anticipate degradation.

However, understanding vegetation patterns offers a solution. Analysing vegetation patterns can give an indication of ecosystem health (Ares, Del Valle & Bisigato, 2003; Barbier et al., 2006; Berdugo et al., 2017). Moreover in the case of catastrophic shifts, vegetation patterns function as early warning signals (Scheffer et al., 2009; Saco et al., 2018), Spatially explicit mathematical models turned out to be very successful in simulating vegetation patterns. The last two decades, mathematical models showed a large potential for understanding the origin and behaviour of dryland dynamics (Bastiaanse et al., 2018; Caviedes-Voullième & Hinz, 2020; Gilad et al., 2007; von Hardenberg et al., 2001; Rietkerk et al., 2002; Meron, 2012). Moreover, modelling work identified early warning signals and signs of degradation (Kefi et al., 2007; Rietkerk et al., 2004) as well as guidelines for restoration (Berghuis et al., 2020). In these works for the formation of regular patterns, but not necessarily for irregular e.g. Kefi et al. (2007), the resource concentration mechanism is assumed the main driving process. Although this scale-depended feedback is widely accepted as cause of regular vegetation patterns, this has not yet been experimentally validated. Regular vegetation patterns in drylands typically occur on a large spatial scale (hectares) and develop on a long temporal scale (decades), making these patterns unsuitable for any kind of manipulative experiments. Vegetation showing similar self-organizing behaviour as observed in drylands, but on a finer spatiotemporal scale could offer an opportunity to address this knowledge gap.

First mentioned in von Hardenberg et al. (2001), later also in e.g. Gilad et al. (2004), Meron et al. (2004), Meron (2011), Rietkerk et al. (2004) and Vincenot et al. (2016). The grass *Paspalum vaginatum* (*P.vaginatum*) is believed to show similar self-organizing behaviour as observed for dryland vegetation (Fig. 1). Forming similar regular patterns as response to increasing drought stress (Fig. 1a), but on a small spatial (10-15 cm) and short temporal (2-3 weeks) scale (von Hardenberg et al., 2001).

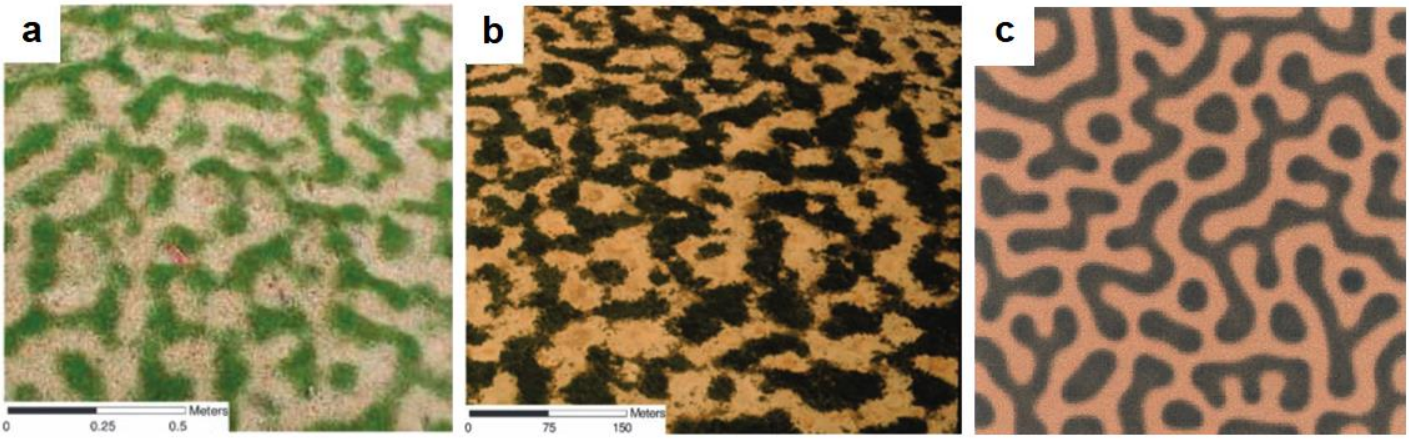

Figure 1 | Three examples of regular vegetation patterns. a) Labyrinth pattern of *P.vaginatum* grass, observed after a period of drought in a residential lawn (Northern Negev, Israel). With 200 mm mean annual rainfall and a typical distance between patches of 10cm (Von Hardenberg et al., 2001). b) Labyrinth pattern of bushy vegetation in Niger with a patch distances around 50m (Rietkerk et al., 2004). c) Labyrinth pattern of vegetation resulting from a frequently used spatial explicit dryland model, the panel has a 400m x 400m scale (Rietkerk et al., 2002).

The fine scale spatial organization of *P.vaginatum* offers the opportunity to recreate regular patterns within a controlled lab setup, similar to those of drylands. In this research we aim to create regular vegetation patterns by executing a manipulative experiment for the first time. In a custom build lab environment, different drought treatments will be imposed on a *P.vaginatum* grass surface. The spatial explicit dynamics of the grass adaptive behaviour will be measured and monitored. Answering the following research question: Can drought stress trigger regular vegetation patterns of *P.vaginatum* and what are the related spatial and temporal dynamics?

We hypothesize that under spatial homogeneous environmental conditions different drought treatments will trigger regular pattern formation of *P.vaginatum* from a homogenous grass surface. Note, homogeneity or 'uniformity' of the driving force as well as the system are of key importance in regular pattern formation, see e.g. Meron (2012). We expect regular pattern formation similar in organization and scale to the picture of figure 1a. The drought treatments in

the experiment will consist of watering only sufficient to support a fraction of the grass surface, triggering patchiness. The regular pattern formation of *P.vaginatum* grass is believed to be driven by the resource concentration mechanism called the root augmentation feedback. Locally, a positive feedback exists between enhanced water uptake and a well-developed root system. Because of lateral growth, well developed root systems can also take up water from the surrounding soil and eventually outcompete neighbouring grass. This scale dependent feedback leads to symmetry breaking of the soil water uptake by the *P.vaginatum* grass surface and the eventual regular pattern formation (Gilad et al., 2004; von Hardenberg et al., 2001; Meron et al., 2004).

Creating self-organized regular vegetation patterns in a controlled experimental setup, can provide the lacking empirical evidence of already widely accepted theories on regular pattern formation in drylands. The results of this kind of experiments are not only relevant for providing empirical evidence of vegetation patterns, but also for calibrating and parameterizing existing mathematical models which predict this phenomena. These 'adjusted/validated' models have the potential to support or even enrich existing insights. This contributes valuable knowledge to better understand the complexity of vegetation patterns, crucial to counter act the large scale land degradation threatening drylands worldwide.

Methods

In this section the methodology used to answer the research question is presented. First the experimental setup described, followed by the experimental design and data analysis. Since the experiment will be a first in its kind, each of the different components of the experimental setup will be described and argumentized as reference.

Experimental setup

The experiments took place in the IBED erosion lab, part of the University of Amsterdam. This lab, previously used for e.g. erosion experiments (Wang et al., 2014), consist of a rainfall simulator installed above a stainless steel fume (3.85m x 1.20m) surrounded by a plastic curtain concealing this environment. The main components added for the experiment of this master thesis are an artificial lighting installation and specific substrate for the grass. Furthermore, the rainfall simulator was adjusted to the settings required, an additional (irrigation) dripping plate was custom build and several measuring devices to monitor the lab setup were installed.

Lighting

In order to provide lighting suitable for the growth of *P. vaginatum*, four 1.20m x 1.0m LED panels were installed at a height of approximately 2 m above the grass canopy. The emission spectrum of the used lighting (Lumatek ZEUS 600W grow lights), is designed to optimize plant growth, preventing light related growth limitations (Jiang, Duncan & Carrow, 2004). At a height of 2 m, with 4 panels, an approximate average Photosynthetic Photon Flux Density (PPFD) of 370 umol/m2/s was expected. The PPFD distribution across the flume was measured with a PAR-meter, confirming the light output and showing an equal distribution. Although a specific light requirement for the experiment was difficult to determine, from previous studies with *P.vaginatum* a Daily Light Integral (DLI) > 15 was estimated to not cause any light related limitations (Hodges et al., 2016; Jiang, Duncan & Carrow, 2004; Russell, Karcher & Richardson, 2020; Zhang et al., 2017). The average 370 umol/m2/s of PPFD measured was combined with a controlled photoperiod of 12 hours per day to result in a DLI of 16.

Substrate

In general *P.vaginatum* is a tolerant species, able to grow in a wide range of environmental conditions and soil properties (Brosnan & Deputy, 2008). Field studies and experimental work with Paspalum show that the use of a specific soil type is mostly of inferior importance (Ntoulas & Nektarios, 2017; Lakanmi & Okusanya, 1990). Therefore, the substrate used in the experiment was particularly designed to facilitate the hypothesized root augmentation feedback. To ensure

fast and extensive root development, coarse sand was used. According guidelines for commercial *P.vaginatum* turf growth (USGA, 2004; Beard 1982; Fry & Huang, 2004), as well as empirical results (Rahayu et al., 2014), coarse sand in the substrate promotes root development. For the grain size of this sand, recommendations by the USGA (2004) were followed. To prevent fast drainage to the bottom and facilitate soil water retention throughout the soil profile, the sand was complemented with fine textured loss soil. Using a concrete mixer these two soil types were mixed into a homogeneous substrate. The clumped loss soil used was crushed and sifted (max diameter 5.6 mm) to prevent heterogeneity in substrate root penetrability. Moreover to prevent contamination, clean (certified) horticultural sand was used. A trade-off between water retention capacity and aeration for fast root development resulted in the substrate composition of table 1. The substrate depth was determined to be 10 cm. Ntoulas et al. (2017) proved a substrate depth of 7,5 to be sufficient for paspalum to grow. Moreover, a limited substrate depth prevents investment in deep rooting systems and pushes towards more laterally extended systems, facilitating the root augmentation feedback.

Table 1 | Substrate composition. Average values for organic matter and texture for two separate analyzed samples.

	Bulk density (g/cm³)	**Organic matter (LOI 375C)**	**Texture**		
			Sand	*Silt*	*Clay*
Sample A	**1.523**	0.52%	85%	12%	3%
Sample B	**1.577**	0.56%	78%	19%	4%

Rainfall simulator

In order to water the grass on a regular basis, an existing rainfall simulator was adjusted for the pre-drought treatment phase. The sprinkler system of the simulator was tested using multiple types of nozzles and assessed on the ability to distribute water homogeneously over the flume, combined with an acceptable rainfall intensity. The Lechler 460 4065E CA000, turned out to be the nozzle delivering the most acceptable distribution with an average rainfall intensity of 37.5 mm/hour. The Christiansen uniformity coefficient, assessing uniformity of sprinkler distribution (Christiansen, 1942), was determined 80%, a good uniformity for a rainfall simulator on this scale (Lassu et al., 2015). Next to the 'spray' (sprinkler) system, for the drought experiment a shift to a more accurate (but also labour intensive) 'drip' system was made (Bowyer-Bower & Burt, 1989). A custom built 1.20 by 0.50m dripping plate, with 500 tubes installed in staggered pattern, was used during the experiment. It could be moved along the length of the flume for watering with varying intensity and high accuracy.

Measurement equipment

Several measuring devices were installed to monitor different variables capturing the spatial and temporal dynamics of potential pattern formation. The specific equipment used and their purpose will be briefly discussed. Firstly, a Time Domain Reflectometry (TDR) system was installed. A computer controlling the TDR system (see Heimovaara, Water & Dekker, 1996) was complemented with newer soil moisture sensors (ZENTRA system), to create 24 data points measuring the volumetric water content (θ) over time. The TDR probes were placed in the middle of each of the different drought treatments. To detect heterogeneity on a *P.vaginatum* pattern scale resolution (10cm), the 4 available sensors per treatment were placed in a line with a 5cm distance. The Zentra sensors were installed to monitor and measure the overall soil water dynamics per treatment and therefore placed on a coarser resolution. Again 4 sensors per treatment, but now equally distributed across the treatments surface (on the corners of a 60 x 64cm rectangular centred within the 120 x 128 cm plot).

To retrieve spatially explicit data on plant health within the grass surface, three cameras capturing different spectral information were installed. Next to visible light, a camera to detect near infrared (NIR) to determine NDVI and one to capture infrared (IR) were present. The NDVI measurements were not used in the results of this experiment and are further described in Appendix A. The visible light was used to estimate the percentage green cover development over time, the IR to detect plant stress which is not (yet) visible. The IR or thermal images display canopy temperature, an indicator of early non-visible plant stress and an excellent substitute for NDVI (Hong, Bremer & van der Merwe, 2019). Canopy temperature has been used for a long time to determine evapotranspiration (ET) (Hatfield, Reginato & Idso, 1984). The ET of healthy plants have a cooling effect, this effect decreases along with plant health (Hatfield, Reginato & Idso, 1984; Anderson et al., 2012). The following cameras were at our disposal: a NIKON D3200 (24.2 mp) and a FLIR b50 (150*150 IR resolution, with 2.3 mp digital camera). The NIKON could be attached to a fixed platform 2m above the centre of the grass surface (between the lighting and watering equipment). For the FLIR, due to its limited field of view (FOV) and hand held shooting, 10 fixed holders were created again at a 2m height. Manually placing the camera in the separate holders created a composite of 10 images, covering the entire flume.

.

Experimental design

Rooting phase

To ensure an homogeneous and dense turf to start the experiment, already matured *P.vaginatum* (variety: *Sealsle* 2000) sods were placed on top of the substrate in the flume, followed by a 40 days rooting phase. In accordance to previous experiments and a mesocosm (with transparent wall) added to monitor root development, within these 40 days *P.vaginatum* could develop a rooting system within the substrate. In this period the grass received infrequent deep watering of a once a week event, watering up to field capacity (soil water content of 20-25%). Starting with a reference to refill total ET, derived from literature recommendations (Huang, 2008), the watering was adjusted using the soil water measurements to reach field capacity.

To ensure nutrients would not become limiting in the rooting phase as well as during the experiment, a one-time addition of 4 g Nm^{-2} (9-3-4 N-P-K) liquid fertilizer was applied (determined from fertilizer use in experiments with similar setup: Gaetani et al., 2017; Jespersen et al., 2019; Ntoulas et al. 2017; Zhou et al., 2012; and general recommendations: USDA, 2004). The fertilizer was distributed homogeneously using a pump sprayer in the first week of the rooting phase.

To recreate lawn conditions (of Fig. 1a), after 20 days the first mowing event took place. Grass was homogeneously mowed using an electric hand trimmer with a 5 cm target height. Since in this case a particular mowing height was found not to be of importance for root development (Elansary & Yessoufou, 2015; Kopec et al., 2007), we choose a common (lawn) mowing height and one comparable to figure 1a. The grass was mowed an additional 3 times with equal intervals, including the last day before the start of the experiment.

Drought treatments

After the rooting phase, in a 45 day experiment, 3 different drought treatments were applied. Aluminium bulkheads divided the flume in 3 equal plots (120cm x 128 cm), preventing any transfer of surface or soil water. Every plot received a different drought treatment, derived from a reference ET. The reference ET for *P.vaginatum* in the specific lab conditions was derived using the soil water data from the last week prior to the experiment. Due to the nature of the lab setup the reference ET could be estimated by using the known water input (P) and the maximum change of soil water content over time (ΔS). Note: because of the closed flume there are no drainage nor runoff components. A simple water balance equation: $ET = P - \Delta S$ (following the conservation of mass), gave a (100%) reference ET of 0.051 L/m2/h. Within the range of the Aridity Index (AI) we choose 3 representative percentages: 12.5 % ET, 25% ET and 50% ET. Respectively within the range of arid, semiarid and subhumid climate conditions (MEA, 2005). Starting after the 14th

day (the first two weeks were allocated for soil water to drop from field capacity to wilting point) the drought treatments consisted of a once a week watering frequency).

Data collection

During the experiment the different variables were measured according to the following. To assess the heterogeneity of the soil water content on a *P.vaginatum* pattern scale resolution (10cm), 4 TDR probes per treatment were placed in a line with a 5 cm distance in the middle of each plot. Due to an defect the measurements of these probes needed to be started manually, and could only be retrieved around the start of the experiment. The Zentra sensors were installed to measure, but also monitor the overall soil water dynamics per treatment. Therefore again 4 sensors per treatment were placed, but now equally distributed within the plot (on the corners of a 60 x 64cm rectangular centred within the 120 x 128 cm plot). The Zentra sensors measured soil water content continuously with a temporal resolution of an hour.

Twice a week visual and thermal pictures were taken to detect regular pattern formation and capture the spatial and temporal dynamics of the grass. The NIKON could be attached to a fixed platform 2m above the centre of the grass surface (between the lighting and watering equipment), covering the main part of the flume. For the FLIR, due to its limited field of view (FOV) and hand held shooting, 10 fixed holders were created again at a 2m height. Manually placing the camera in the separate holders created a composite of 10 images, covering the entire flume. Pictures were always taken prior to watering events on coinciding dates.

Data analysis

Since most data was gathered in the form of pictures containing spectral information per pixel, some additional processing and analysis was required. The following methodology was used to quantify the average development of the variables in the pictures over time as well as quantify spatial distribution.

The pictures capturing the visual spectrum were used to analyse the change in green cover over time as well as the spatial distribution of green and dormant areas. In order to quantify green cover, a case specific spectral definition for 'green cover' needed to be established. An picture of the grass surface at the end of the rooting phase was used as reference (Appendix B). In this image all the shades of green present in a substantial amount, after filtering out small background areas between the grass blades, were considered 'green'. This resulted in the following (RGB) thresholds (For the *FLIR* camera: R 75-135, G 85-170, B 0-127. For the *NIKON* camera: R 35-112, G 55-255, B 0-255). With these thresholds, RGB images could be transformed in a binary matrix of green and non-green (dormant) pixels. For the threshold selection a *color thresholder* app was used. The binary images were retrieved using an adjusted *color detection* code, where the color thresholds were applied on the images of the grass cover. Both analyses were executed in Matlab R2019a. The binary matrices from the *FLIR* camera were used as input for total green cover calculation (sum of the green pixels as fraction of total pixels). The more detailed binary matrices from the *NIKON* camera were used for the spatial distribution analyses. In order to detect and quantify only the spatial heterogeneity on a pattern scale resolution, the binary images were coarse-grained such that small scale background heterogeneity was filtered out. After, the degree of spatial aggregation of green and dormant pixels was identified with a (lag-1) spatial autocorrelation measured by Moran's *I* (Legendre & Fortin, 1989). The statistical significance of this coefficient was tested, and moreover corrected for a changing (green) cover of the different images. This resulted in spatial aggregation quantified in a (statistically significant) cover corrected Moran's *I* 'z-score'. For this spatial autocorrelation analysis a section of the *spatial warnings* R-package of Génin et al. (2018) was used. The analysis was executed in RStudio. The thermal images taken of the grass surface needed less processing, besides the usual cropping and rearranging. From the images, using FLIR tool software, data matrices with temperature values per pixel could be retrieved. With these matrices average temperature could be computed, and the matrices were used as input for the spatial autocorrelation analysis. For the spatial autocorrelation a similar analysis took place as for the green cover, again using the *spatial warnings* R-package of Génin et al. (2018), and quantified in the earlier defined Moran's *I* 'z-score'.

Results

Regular pattern formation

Following a successful experiment, for all drought treatments, no regular patterns in the green cover of *P.vaginatum* similar to those of figure 1 could be observed. The grass did not decay homogeneously, but in the patchiness formed there were no signs of any regularity. All spatial heterogeneity in the grass canopy, on the scale of the expected patterns, was considered irregular. Figure 2 shows the average development of the measured variables during experiment. Figure 3 and 4 show the spatial explicit dynamics, the spatial aggregation of green cover (Fig. 3) as well as of differences in canopy temperature (Fig. 4).

Spatial and temporal dynamics

Starting with the total percentage green cover (Fig. 2b), the 12,5% ET and 25% ET drought treatments resulted in a complete loss of green cover when passing 30 days of drought. Looking at the spatial development corresponding to these drought treatments in figure 3a, the decay of green cover did not occur homogeneously. After the first 10 days of homogenous green cover, healthy green and decaying dormant grass start to cluster (Fig. 3). However this clustering does not stabilize, leading to a homogeneous dormant cover around 30 days. Note, homogenous cover, whether green or dormant, results in spatial aggregation values close to zero, while patchiness gives high values, explaining the non-monotonic shapes in figure 3. In contrast to the 12,5% and 25%, the 50% ET treatment did not completely decay, sustaining a substantial green cover throughout the experiment (Fig. 2b). The overall green cover decreases more gradually for 50%ET (Fig. 2b), accompanied by a clustering of green and dormant grass which lasts longer (Fig. 3). From the current time span it is difficult to assess whether the patchiness for the 50% ET treatment could stabilize. For 50% ET (and to a lesser degree for 25% ET), a clear response to the watering events is visible, causing a temporary rise in the average ‘greenness’ (Fig. 2b).

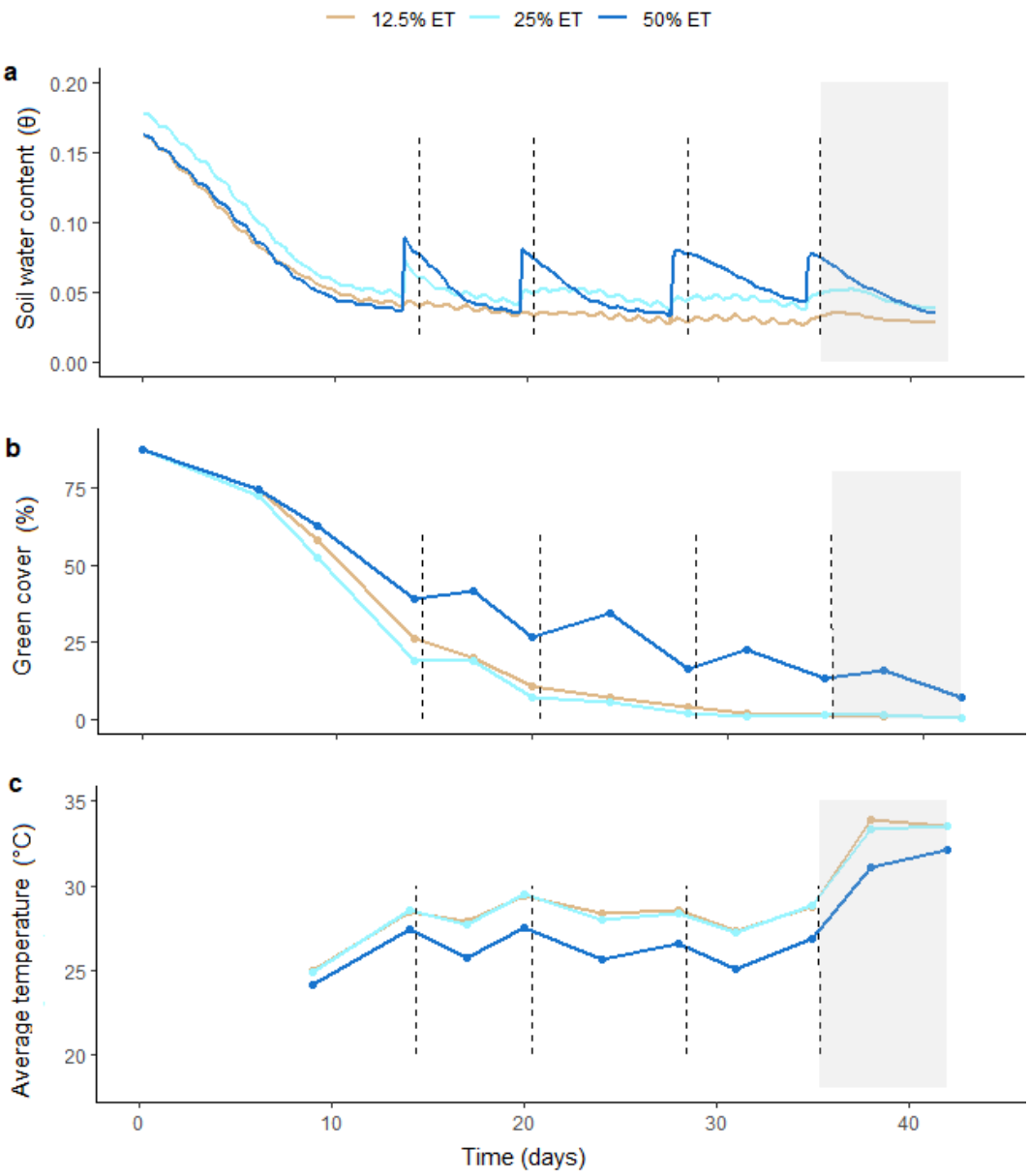

Figure 2 | Overall development of the measured variables for the different drought treatments. The dashed lines indicate the weekly watering events, with the watering intensity varying per treatment. **a)** The average soil water content determined on an hourly basis throughout the experiment. **b)** The development of the total percentage green cover, determined for images taken twice a week. **c)** The average temperature of the grass surface, again determined for images taken twice a week. Note, the data points for green cover and average temperature lie always just before, when close to, a watering event. The grey shade indicates the anomaly in air temperature for the last week.

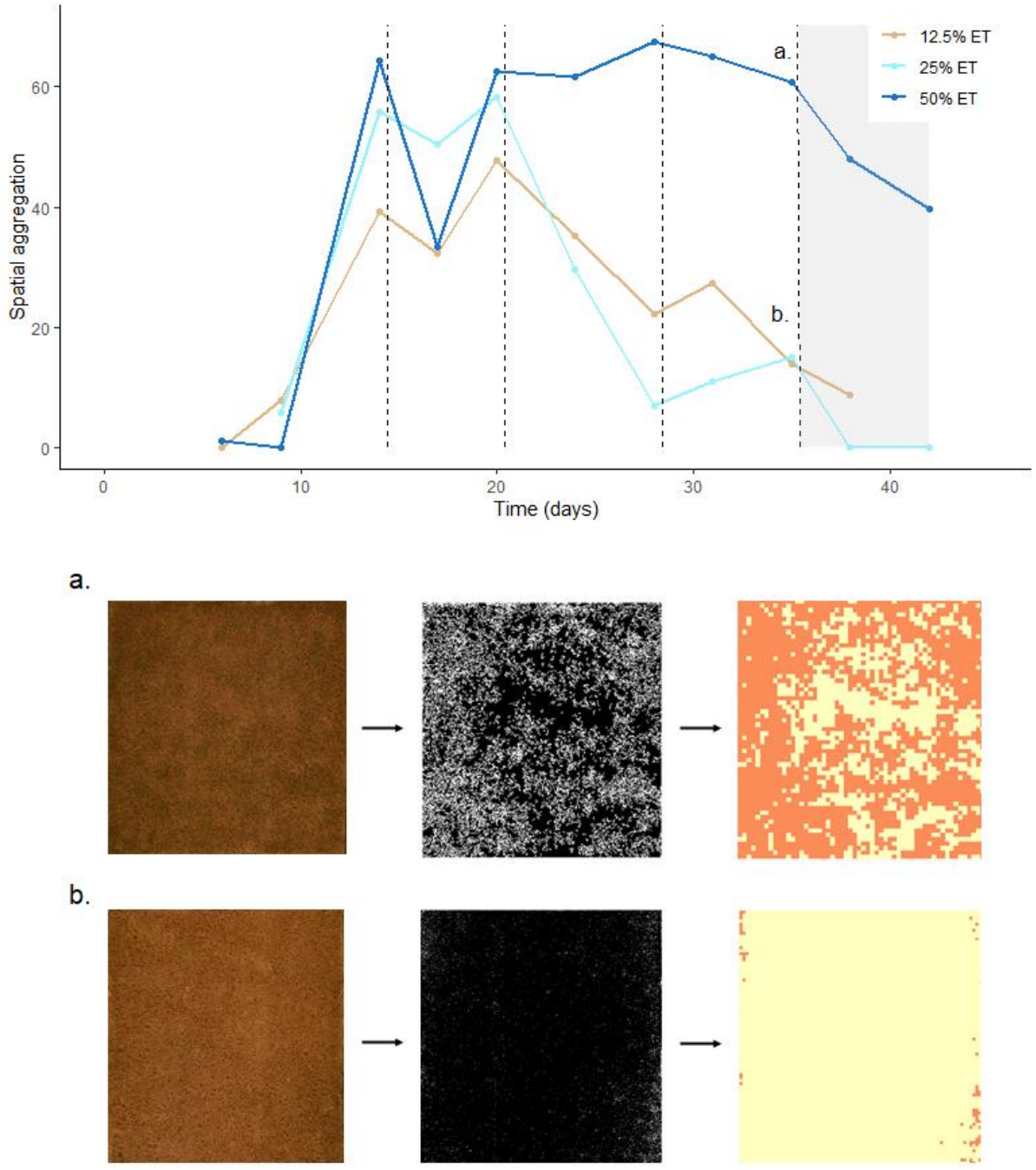

Figure 3 | The spatial aggregation of green cover for the different drought treatments. The spatial aggregation is quantified for a cover corrected Morans I score. The dashed lines indicate the weekly watering events, with the watering intensity varying per treatment. Two data points in the graph are highlighted and visualized in the lower panel. **a.,b.)** Two examples of green cover pictures and their binary and coarse grained equivalents (see method for the processing procedure). a.) Green cover on day 35 for the 50% ET treatment. b.) Green cover on day 35 for the 25% ET treatment.

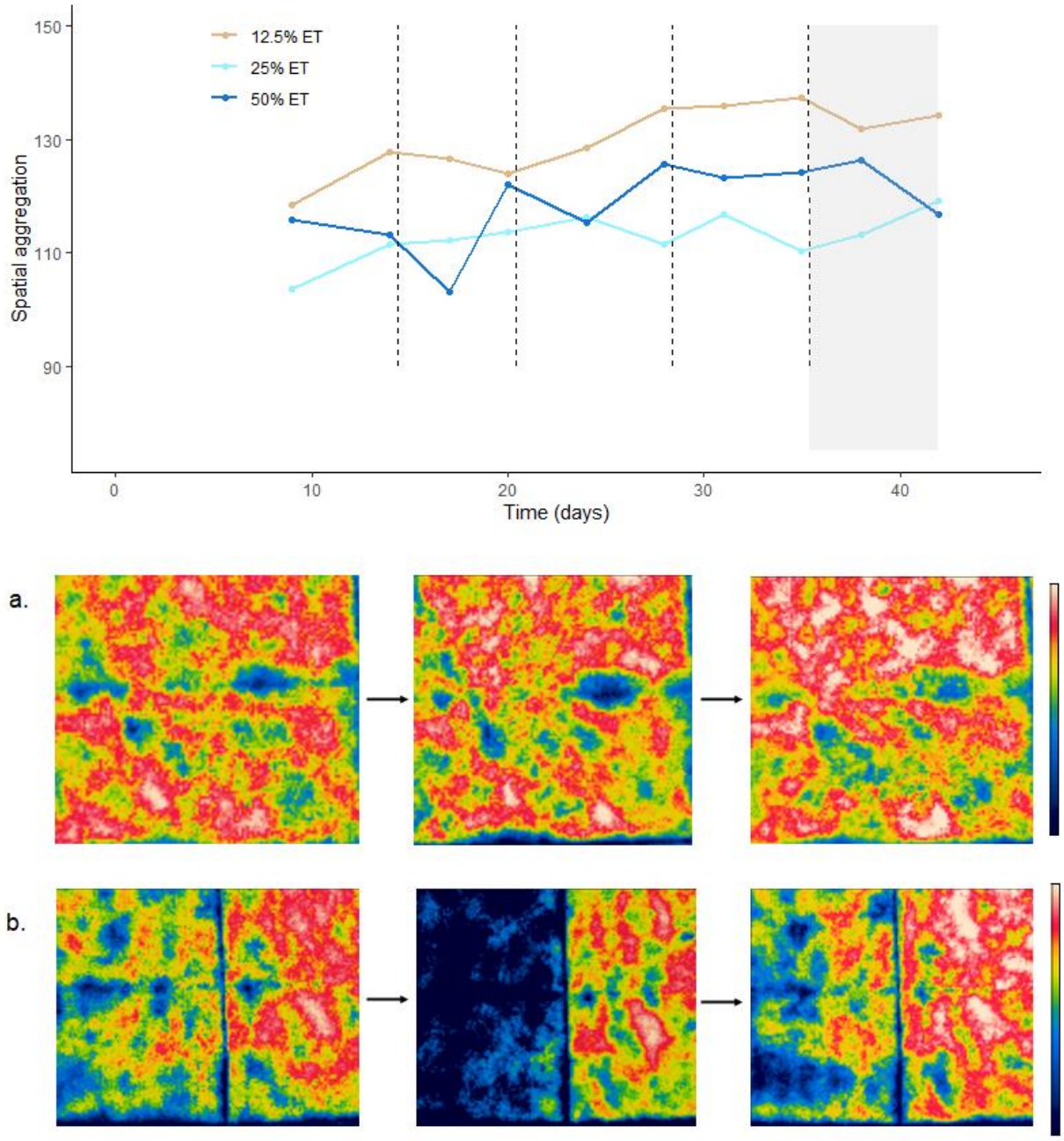

Figure 4 | The spatial aggregation of differences in canopy temperature for the different drought treatments. The spatial aggregation is quantified for a cover corrected Moran's I score. The dashed lines indicate the weekly watering events, with the watering intensity varying per treatment. In the lower panel the patterns in canopy temperature are visualized for two areas. The colour bar has a minimum of 26 and maximum of 30 degrees Celsius. **a.)** The thermal pattern for the 12.5 %ET treatment in the lower corner of the plot. For respectively day 14,24 and 35. **b.)** The thermal pattern at the boundary of the 25% ET (right) and the 50 %ET (left), for again respectively day 14,24 and 35. Note the sharp boundary between the different treatment, and difference in overall temperature. Since the temperature scale is constant for comparing the plots, it has an effect on the rate of distinctiveness of the patterns depending on the range of overall average temperature (Fig. 2c).

For the spatial distribution of the grass surface's canopy temperature (Fig. 4) a constant high degree of spatial aggregation is present for all three drought treatments. This high spatial aggregation results from a patchy pattern of relatively high and low canopy temperatures in the grass surface (Fig. 4). These patches have a similar scale, but are more distinctive and more evenly organized compared to the patchiness in green cover, translating in the higher degree of spatial aggregation (Fig. 3 and 4). The spatial aggregation is highest for the 12,5% ET treatment, the 25% ET and 50% ET treatments fluctuate more, but in general the spatial aggregation is higher for 50% ET. The average canopy temperature for the drought treatments (Figure 2c), is clearly lower for 50% ET, and similar for 12,5% ET and 25% ET. The fluctuation in temperature seems to be related to the watering events, where a watering event has a temporarily cooling effect. Figure 4 visualizes the sharp boundary in canopy temperature per drought treatment. In the last two weeks an evident increase in canopy temperature for all drought treatments occurred (Fig. 2c), this was related to an increase in air temperature (Appendix C), caused by a defect in the lab's air circulation.

Soil water content was used to monitor the drought treatments in this experiment, and as expected reacted proportional and consistent to the watering events (Fig 2a). The first 14 days show a sharp depletion of soil water, dropping from the field capacity at the end of the rooting phase to the wilting point just before the first watering event. After the following watering events, soil water content reacted proportional to the different treatments. Since water was the limiting factor in this drought experiment, the trend of the soil water dynamics can be recognized for the other variables (Fig. 2,3 and 4). However, the impact of decreasing green cover does also affect soil moisture, as with decreasing photosynthetic activity soil moisture decline slows down after watering (evident for 25% ET, Fig. 2a). In order to give an indication of the spatial heterogeneity of the soil moisture, figure 5a presents the average standard deviations between the different measuring points within the same drought treatment. The spatial variance of soil moisture was largest within the 50% ET treatment, 12.5 % ET and 25% ET are more similar, with the latter having the lowest spatial variance during the experiment (Fig. 5a). Figure 5b shows the spatial variance of the sensors placed on the finer 5cm resolution. Although measured for a limited period and less frequent, figure 5b indicates the spatial variance of figure 5a potentially underestimates the variance on a pattern scale resolution. Note, figure 5 shows the average spatial variance, including values in time were spatial heterogeneity is not expected (just before and after the watering events). Overall, the distribution presented in the boxplots show a substantial amount of heterogeneity in soil water content varying over time.

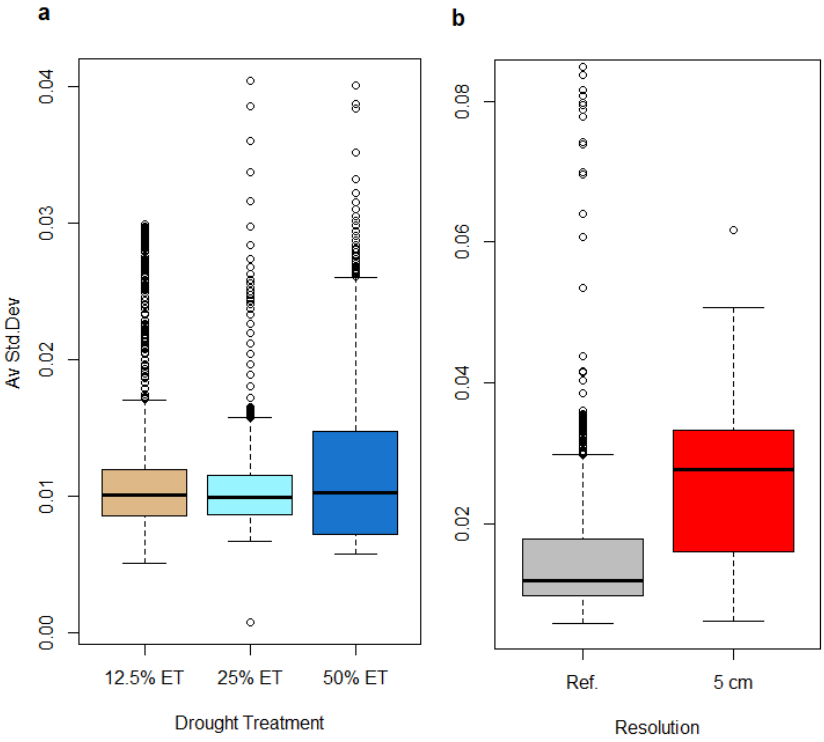

Figure 5 | The spatial heterogeneity in the measured soil water content. a) The average standard deviation of the soil moisture measurements within the same drought treatments. Computed for on an hourly basis throughout the experiment (N =4). **b)** Again the average standard deviation of the soil moisture measurements, but now for a different spatial resolution. The 5cm resolution represents the standard deviation of the combined sensors installed in the middle of each drought treatment (N = 12). The grey boxplot functions as reference, presenting the combination of the standard deviations of the treatments of 5a for the similar measuring period of the 5cm resolution data.

Because soil water content and canopy temperature share a similar level of plasticity to drought treatments (e.g. compared to the delayed response in time for canopy greenness), their dynamics could be compared in an additional analysis. In this point sample analysis, the measured data of both variable are compared for the same moment in time and space. For 40 different points in throughout the experiment, the values measured for both variables were compared using a Spearman's rank-order correlation. The known locations and size of the measurement area of the soil moisture sensors belowground were compared to corresponding aboveground (average) canopy temperature, clipped out for the same area . The analysis shows no clear correlation for the 12.5% ET and 25% ET treatments. The 50%ET has a more clear relation, where significantly, a higher canopy temperature often comes with a lower soil water content belowground (Spearman's rho (r_S) = -0.31, $p < 0.1$; r_S = - 0.19, $p < 0.5$; r_S = - 0.58 $p < 0.0001$, for respectively 12,5% ET, 25% ET and 50% ET).

Discussion

This study was motivated by the observation of fine scale regular patterns of *P.vaginatum* in the field, as well as by what suggested in modelling studies. It was hypothesized that similar to large scale dryland systems, a scale dependent feedback would apply for *P.vaginatum* and form regular patterns as reaction to drought stress. Despite a successful experiment, the different drought treatments did not result in the expected regular pattern formation. Looking at the spatial and temporal dynamics captured during the experiment, the grass did not show a uniform decay. *P.vaginatum* showed a substantial degree of spatial aggregation, clustering in green and dormant cover. This spatial aggregation had a transitional nature and did not stabilize (at least for 12,5% ET and 25% ET). Measurements of the canopy temperature showed a higher degree of spatial aggregation. Patches of high and low temperature were present for all treatments, forming consistent structured patterns throughout the experiment. Soil water content showed a substantial degree of spatial heterogeneity for different spatial resolutions.

Regular pattern formation

The drought treatments of this experiment did not prove to be successful in triggering regular pattern formation. It is known that the formation of regular patterns in drylands is reserved for a certain range of environmental conditions (von Hardenberg et al., 2001; Berdugo et al., 2019), and can be one of multiple stable states (Bastiaanse et al., 2018). An external pressure can break the resilience of a system (Ingrisch & Bahn, 2018), in such a way that a healthy system with homogenous plant cover shifts to a degraded non vegetated state, without stabilizing at intermediate states e.g. a patchy patterned state (see also catastrophic shift, Scheffer et al., 2001). Looking at the trajectory of the 12,5% ET and 25% ET treatments (Fig. 2b), drought stress was too severe, resulting in a fast transition from a homogeneous green to a homogeneous dormant cover, without stabilizing in the intermediate patchy state. The similar trajectories for 12,5% ET and 25% ET, despite different water availability, support the idea of a broken resilience and abrupt transition. The less extreme 50% ET treatment did show a tendency to stabilize at an intermediate patchy state, however the timespan of the experiment was too short to confirm this stabilization. The 10-20% green cover range corresponding to this potential stabilization, indicates 50% ET is on the lower part of a suitable range, comparable to a spot pattern in dryland systems (Meron et al., 2004).

The observation of regular patterns of *P.vaginamtum* in figure 1a is recorded as a consequence of increasing drought stress. Although for the 50% ET treatment it is not certain (since it did not stabilize), none of the broad range drought stress triggered regular patterns in the performed experiment. Although not focused on pattern formation, other experiments

inducing drought on a substantial surface of *P.vaginatum*, also present no records of any form of regular patterns (Ntoulas & Nektarios, 2015; Jespersen et al., 2019; Pessarakli, 2017; Bañuelos et al., 2011). This implies there could be an alternative explanation for the regular pattern of figure 1a. Although not recorded as such and at first sight unlikely in the climate of the Negev desert, we want point at the alternative explanation of 'chill damage'. A single cold (near freezing) night could already suffice in causing selective chill damage in a grass surface. First described by Thompson & Daniels (2010), instability in fluid dynamics can cause regular patterns of chill damage which are morphologically indistinguishable from those observed in drylands (Fig. 1b). Chill damage has been proven to create regular patterns in warm season grasses, similar to *P.vaginatum*, in field as well as using convection models by Thompson & Daniels (2010) and later by Ackerson, Beier & Martin (2015).

Because of the homogenous conditions during the experiment, the grass can be expected to react uniformly to drought, acting as one system. However the spatial aggregation showed in the results, the clustering of green and dormant areas (Fig. 3), does not entail the expected regularity from a system response driven by the hypothesized root augmentation feedback (Gilad et al., 2004; von Hardenberg et al., 2001; Meron et al., 2004). A possible explanation could lie in the dispersal of *P.vaginatum*. By producing stolons and rhizomes, *P.vaginatum* spreads through clonal reproduction (Fabbri, Perreta & Rua, 2016; Goad et al., 2021). In our experiment, the dense grass turf was highly connected, with rhizomes and ramets present from the beginning. As a reaction to increasing drought stress, *P.vaginatum* was even observed to increasingly invest in explorative ramets (Appendix A). The explorative nature of clonal reproduction is known to produce self-organized patterns triggered by e.g. drought, in several plant communities including grasses (Benot et al., 2013; Couteron et al., 2014; Herben & Hara, 2003). However, driven by an opposite mechanisms compared to regular vegetation patterns in drylands. A mechanism that not adapts, but works opposite to desertification, colonizing areas where vegetation is absent (Bordeu et al., 2016). In this experiment, starting with a dense turf, the aboveground connectivity due to clonal reproduction could counteract regularity in canopy patterns. It interferes with the belowground mechanisms (root augmentation feedback), by spatially allocating resources through the rhizomes (Fabbri et al., 2016; Cornelissen et al., 2014). Although the extensive and lateral root growth makes *P.vaginatum* suitable to facilitate a root augmentation feedback, the combination with the clonal reproduction trait, and the ability of this trait to drive alternative spatial organization, is not favourable for recreating regular patterns.

Spatial and temporal dynamics

The spatial aggregation in canopy temperature is higher and more consistent than measured for green cover (Fig 3b). Although the thermal patterns are not regular, the patchy structure has a similar scale (5-15cm) and rate of organization compared to the regular *P.vaginatum* pattern presented in Fig. 1a. The spatial aggregation of Fig. 1a was determined according the same methodology as for the thermal pictures. This resulted in a similar level of spatial aggregation as presented in figure 4 (a cover-corrected Moran's I of 128). Canopy temperature is in this study approached as an indicator for ET (and therefore plant health). Changes in canopy temperature, as result of decreased plant health, are detected before any visible signs of plant stress (Hong et al., 2019). Although one would expect the thermal patterns over time to be reflected in the green cover distribution, this was not the case. One factor playing a role could be the limited plasticity of canopy greenness reacting to stress compared to the instantaneous and measured response of canopy temperature. Moreover, spatial heterogeneity in the level of drought stress could be reflected in the canopy temperature, but not be strong enough to influence canopy greenness. This could explain the stabilized dormant cover for 12,5% ET and 25%ET, where heterogeneity in canopy temperature is still present (Fig 2b,4). The severeness of the drought treatment is dominant in enforcing overall dormancy, but because of some water availability, local heterogeneity in canopy temperature occurs. Note, in dormant grass a low rate ET can still be present (Doležal et al., 2018). Soil water showed substantial spatial heterogeneity between the limited measurement points throughout the experiment, potentially the source of the spatial heterogeneity in green cover an canopy temperature. The point sample analyses between soil water content and aboveground canopy temperature showed however no clear correlation, except for the 50% ET treatment (where higher temperatures related to less soil water). Following conventional dryland models, where soil water content is strongly related to above ground vegetation (Gilad et al., 2004; Rietkerk et al., 2002), a high correlation between soil water concentration and low canopy temperature could be expected for all the treatments.

Recommendations

In order to provide recommendations for future research, the performance of the experimental setup will be shortly assessed. The rooting phase was considered successful (although no destructive (root) measurement could be taken). In a total of 5 weeks, the grass reached a homogeneous green and healthy cover. From the start of the experiment no other stress, e.g. fungi or cold, than drought induced was visually observed. Moreover, the external conditions were able to be kept relatively constant and homogeneous across the grass surface. This except from the air temperature for the last 7 days, which illustrated the importance of constant conditions. The different drought treatments were applied successfully, resulting in three separate systems.

However, the induced drought stress for 12,5% ET and 25% ET was considered too severe, as this resulted in a relatively fast stabilization of a uniform dormant state. The 50% ET treatment had more potential to support a stable patchy system, and potentially lies (in the lower part) of a suitable range. The length of the experiment (45 days) turned out to be insufficient for the system to stabilize in a patchy state, evident for the 50% ET treatment . Although the analyzation of plant performance using green cover (%) offered valuable insights, it proved not sufficient. An additional indicator with a higher plasticity (faster response) should be added, suitable for assessing the relation of plant health to the dynamics of the other variables (e.g. the thermal patterns) on a fine temporal resolution. An indicator of plant health not only based on the relatively inert canopy greenness, e.g. NDVI could be added (Note the complications of indoor lighting conditions for NDVI, Appendix A).

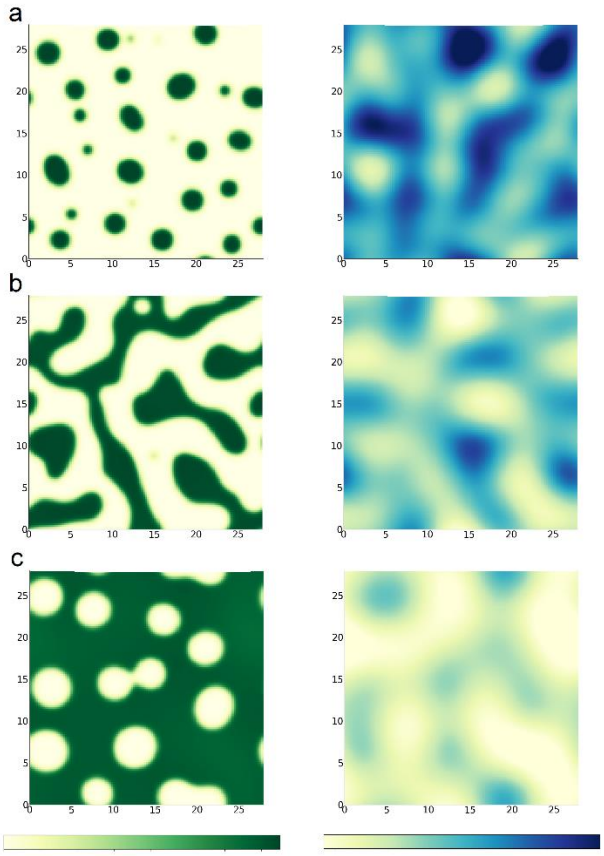

Figure 6 | Modelling results from the adjusted model of Gilad et al. (2004). For three different values of non-dimensional precipitation (p) the Vegetation density (left) and the corresponding soil water concentration (right) are given With for a,b and c, respectively p = 2, p = 5 and p = 8. Non-dimensional running time for all plots t =50 (-). Colour bar's for vegetation density and soil water concentration have a range of 0 - 0.75 and 0 - 0.105 respectively.

To translate the insights from the empirical results of this study to recommendations for future modelling work, an adjusted version of the model of Gilad et. (2004) by J.von Hardenberg and M.Baudena will be used. The infiltration and shading feedback of the original model were removed, as although of importance in dryland systems, for a more representative comparison with the experiment, only the root augmentation feedback should be present. Since the model of Gilad et al. (2004) is built to simulate vegetation patterns for large scale dryland systems, the model was adjusted to be 'scale free' by nondimensionalizing the equations (similar to Gilad et al., 2007). Figure 7 presents 3 different organizations of vegetation patterns for different non-dimensional values of precipitation (p). Figure 6 illustrates that from a modelling perspective, with only the root augmentation feedback present, regular vegetation patterns can form independent of the scale of the system. A possible explanation for the discrepancy between these model simulations and the experimental results could lie in the quantification of plant dispersal in the model. In dryland models plant dispersal (including clonal reproduction) is often described with a diffusion term. This is also the case in Gilad et al. (2004). Note that diffusion is metric (equally dispersing in all directions), and 'flows' (expanding from existing vegetation, not able to 'jump' in space). On a larger system scale (with a patch resolution of e.g. 50m, Fig. 1b), diffusion approximates different types of local plant dispersal. However, on a finer scale this approximation becomes inaccurate. In the case of this experiment, the spatial scale of the foraging behaviour of clonal reproduction (Cain, Dudle & Evans, 1996), transcends the pattern scale of *P.vaginatum*. As proposed earlier in this discussion, supported by the experimental results, for the clonal reproduction of *P.vaginatum* this can result in a different spatial distribution of vegetation. In the case of clonal reproduction, but potentially also for other dispersal traits (Thompson, Katul & McMahon, 2008).

Figure 6 also shows the soil water distribution corresponding to the above ground vegetation. Soil water seem to be more depleted near vegetation patches, but more importantly does not follow the distribution of the above ground vegetation. Figure 6 confirms what is already indirectly implied in Gilad et al. (2007), the 'shading' and 'infiltration' feedback cause the higher concentration of soil water beneath vegetation patches. The root augmentation feedback also transports soil water to the vegetation patches, however via roots, and therefore this resource concentration is not indicated by higher soil water distribution beneath the canopy. The conventional interpretation of soil water concentration beneath regular vegetation patches indicating eco engineering strength (e.g. Rietkerk et al., 2002; Gilad et al., 2004; Gilad et al., 2007), should therefore be adjusted here. This lies also in line with the heterogeneity found for soil water content in the experiment, but the lack of a clear (negative) spatial correlation to canopy temperature (and therefore indirectly plant health).

Adjusting the model of Gilad et al. (2004) showed that pattern formation still occurs with solely a root augmentation and independent of spatial scale. However, case specific mechanism should be included. It is strongly recommended that on a finer spatial scale, plant dispersal is not represented by a general diffusion, but more plant specific term. Also, the interpretation of soil water distribution strongly depend on the case specific feedback mechanism present. These recommendations fit well with the line of argumentation recently presented in a review of Martinez-Garcia et al. (2021). Stressing the importance of models correctly capturing the specific mechanisms at play, rather than focusing on the simulation of phenomenological identical vegetation patterns. This, to eventually provide more useful and reliable ecological predictions.

Conclusion

In contrast to what was hypothesized based on field observations and model predictions, the presented experiment did not result in regular patterns of *P.vaginatum*. The different drought treatments did not trigger the expected system response within the spatial scale and temporal scope of this experiment. Besides the absence of regularity, within the environmental homogeneous conditions a large degree of spatial heterogeneity in the green cover as well as canopy temperature of *P.vaginatum* was captured. The analysis of the measured spatial heterogeneity offered new information on the spatial patterning of *P.vaginatum* adapting to different levels of drought. Moreover, the experiment sheds new light on the interpretation of regular patterns observed for *P.vaginatum*, and offers insights and recommendations for the translation of dryland modelling to a finer spatial scale. The experiment presented in this master thesis offers a starting point for future efforts trying to provide the empirical evidence for dryland models, leading to the eventual model parameterization and calibration crucial for the accurate monitoring and prediction of dryland degradation.

Acknowledgements

First of all I want to say a special thank you to my supervisor Angeles, for all the enthusiasm and support, and to Erik, for all the help in the lab and devoting his time to this project.

I also want to thank Max and Mara for the sparring sessions, Jost for adjusting the model, Alex for his input on the spatial analysis, Rutger for the technical support in the lab and Daniel for the lighting equipment.

References

Ackerson, B. J., Beier, R. A., & Martin, D. L. (2015). Ground level air convection produces frost damage patterns in turfgrass. *International journal of biometeorology*, *59*(11), 1655-1665. https://doi.org/10.1007/s00484-015-0972-3

Aguiar, M. R., & Sala, O. E. (1999). Patch structure, dynamics and implications for the functioning of arid ecosystems. *Trends in Ecology & Evolution*, *14*(7), 273-277. https://doi.org/10.1016/S0169-5347(99)01612-2

Anderson, M. C., Allen, R. G., Morse, A., & Kustas, W. P. (2012). Use of Landsat thermal imagery in monitoring evapotranspiration and managing water resources. *Remote Sensing of Environment*, *122*, 50-65. https://doi.org/10.1016/j.rse.2011.08.025

Ares, J., Del Valle, H., & Bisigato, A. (2003). Detection of process-related changes in plant patterns at extended spatial scales during early dryland desertification. *Global Change Biology*, *9*(11), 1643-1659. https://doi.org/10.1046/j.1365-2486.2003.00690.x

Bañuelos, J. B., Walworth, J. L., Brown, P. W., & Kopec, D. M. (2011). Deficit irrigation of seashore paspalum and bermudagrass. *Agronomy journal*, *103*(6), 1567-1577. https://doi.org/10.2134/agronj2011.0127

Barbier, N., Couteron, P., Lejoly, J., Deblauwe, V., & Lejeune, O. (2006). Self-organized vegetation patterning as a fingerprint of climate and human impact on semi-arid ecosystems. *Journal of Ecology*, *94*(3), 537-547. https://doi.org/10.1111/j.1365-2745.2006.01126.x

Bastiaansen, R., Jaïbi, O., Deblauwe, V., Eppinga, M. B., Siteur, K., Siero, E., ... & Rietkerk, M. (2018). Multistability of model and real dryland ecosystems through spatial self-organization. *Proceedings of the National Academy of Sciences*, *115*(44), 11256-11261. https://doi.org/10.1073/pnas.1804771115

Beard, J.B. 1982. Turf management for golf course. Macmillan Pub-lishing Company, NY, USA. p. 642.

Benot, M. L., Bittebiere, A. K., Ernoult, A., Clement, B., & Mony, C. (2013). Fine-scale spatial patterns in grassland communities depend on species clonal dispersal ability and interactions with neighbours. *Journal of Ecology*, *101*(3), 626-636. https://doi.org/10.1111/1365-2745.12066

Berdugo, M., Kéfi, S., Soliveres, S., & Maestre, F. T. (2017). Plant spatial patterns identify alternative ecosystem multifunctionality states in global drylands. *Nature ecology & evolution*, *1*(2), 0003. https://doi.org/10.1038/s41559-016-0003

Berdugo, M., Soliveres, S., Kéfi, S., & Maestre, F. T. (2019). The interplay between facilitation and habitat type drives spatial vegetation patterns in global drylands. *Ecography*, *42*(4), 755-767. https://doi.org/10.1111/ecog.03795

Berghuis, P. M., Mayor, Á. G., Rietkerk, M., & Baudena, M. (2020). More is not necessarily better: The role of cover and spatial organization of resource sinks in the restoration of patchy drylands. *Journal of Arid Environments*, *183*, 104282. https://doi.org/10.1016/j.jaridenv.2020.104282

Bestelmeyer, B. T., Okin, G. S., Duniway, M. C., Archer, S. R., Sayre, N. F., Williamson, J. C., & Herrick, J. E. (2015). Desertification, land use, and the transformation of global drylands. *Frontiers in Ecology and the Environment*, *13*(1), 28-36. https://doi.org/10.1890/140162

Bordeu, I., Clerc, M. G., Couteron, P., Lefever, R., & Tlidi, M. (2016). Self-replication of localized vegetation patches in scarce environments. *Scientific reports*, *6*(1), 1-11. https://doi.org/10.1038/srep33703
Bowyer-Bower, T. A. S., & Burt, T. P. (1989). Rainfall simulators for investigating soil response to rainfall. *Soil technology*, *2*(1), 1-16. https://doi.org/10.1016/S0933-3630(89)80002-9

Brosnan, J. T., & Deputy, J. (2008). Seashore Paspalum: Turf Management. *TM-1, Mānoa, Hawaii: University of Hawaii at Mānoa, 8p*.

Cain, M. L., Dudle, D. A., & Evans, J. P. (1996). Spatial models of foraging in clonal plant species. *American Journal of Botany*, *83*(1), 76-85. https://doi.org/10.1002/j.1537-2197.1996.tb13877.x

Caviedes-Voullième, D., & Hinz, C. (2020). From nonequilibrium initial conditions to steady dryland vegetation patterns: How trajectories matter. *Ecohydrology*, *13*(3), e2199. https://doi.org/10.1002/eco.2199

Christiansen, J. E. (1942). *Irrigation by sprinkling* (Vol. 4). Berkeley: University of California.
clonality: a new research agenda. *Annals of botany*, *114*(2), 369-376. https://doi.org/10.1093/aob/mcu113

Cornelissen, J. H., Song, Y. B., Yu, F. H., & Dong, M. (2014). Plant traits and ecosystem effects of

Couteron, P., Anthelme, F., Clerc, M., Escaff, D., Fernandez-Oto, C., & Tlidi, M. (2014). Plant clonal morphologies and spatial patterns as self-organized responses to resource-limited environments. *Philosophical Transactions of the Royal Society A: Mathematical, Physical and Engineering Sciences*, *372*(2027), 20140102. https://doi.org/10.1098/rsta.2014.0102

D'Odorico, P., Bhattachan, A., Davis, K. F., Ravi, S., & Runyan, C. W. (2013). Global desertification: drivers and feedbacks. *Advances in water resources*, *51*, 326-344. https://doi.org/10.1016/j.advwatres.2012.01.013

D'Odorico, P., Rosa, L., Bhattachan, A., & Okin, G. S. (2019). Desertification and land degradation. In *Dryland ecohydrology* (pp. 573-602). Springer, Cham. https://doi.org/10.1007/978-3-030-23269-6_21

Deblauwe, V., Barbier, N., Couteron, P., Lejeune, O., & Bogaert, J. (2008). The global biogeography of semi-arid periodic vegetation patterns. *Global Ecology and Biogeography*, *17*(6), 715-723. https://doi.org/10.1111/j.1466-8238.2008.00413.x

Doležal, F., Hernandez-Gomis, R., Matula, S., Gulamov, M., Miháliková, M., & Khodjaev, S. (2018). Actual evapotranspiration of unirrigated grass in a smart field lysimeter. *Vadose Zone Journal*, *17*(1), 1-13. https://doi.org/10.2136/vzj2017.09.0173

Elansary, H. O., & Yessoufou, K. (2015). Growth regulators and mowing heights enhance the morphological and physiological performance of Seaspray turfgrass during drought conditions. *Acta Physiologiae Plantarum*, *37*(11), 1-11. https://doi.org/10.1007/s11738-015-1986-5

Eldridge, D. J., Zaady, E., & Shachak, M. (2000). Infiltration through three contrasting biological soil crusts in patterned landscapes in the Negev, Israel. *Catena*, *40*(3), 323-336. https://doi.org/10.1016/S0341-8162(00)00082-5

Fabbri, L. T., Perreta, M., & Rua, G. H. (2016). Spatial structure and development of Paspalum vaginatum (Poaceae): an architectural approach. *Australian Journal of Botany*, *64*(2), 153-159. https://doi.org/10.1071/BT15156

Fry, J., & Huang, B. (2004). *Applied turfgrass science and physiology*. John Wiley & Sons.

Gaetani, M., Volterrani, M., Magni, S., Caturegli, L., Minelli, A., Leto, C., ... & Grossi, N. (2017). Seashore paspalum in the Mediterranean transition zone: phenotypic traits of twelve accessions during and after establishment. *Italian Journal of Agronomy*, *12*(2). https://doi.org/10.4081/ija.2017.808

Génin, A., Majumder, S., Sankaran, S., Danet, A., Guttal, V., Schneider, F. D., & Kéfi, S. (2018). Monitoring ecosystem degradation using spatial data and the R package spatialwarnings. *Methods in Ecology and Evolution*, *9*(10), 2067-2075. https://doi.org/10.1111/2041-210X.13058

Gilad, E., von Hardenberg, J., Meron, E., Shachak, M., & Zarmi, Y. (2004). A Dynamical System Approach to Aridity and Desertification. In *Continuum Models and Discrete Systems* (pp. 405-418). Springer, Dordrecht. https://doi.org/10.1007/978-1-4020-2316-3_64

Gilad, E., von Hardenberg, J., Provenzale, A., Shachak, M., & Meron, E. (2007). A mathematical model of plants as ecosystem engineers. *Journal of Theoretical Biology*, *244*(4), 680-691. https://doi.org/10.1016/j.jtbi.2006.08.006

Goad, D. M., Baxter, I., Kellogg, E. A., & Olsen, K. M. (2021). Hybridization, polyploidy and clonality influence geographic patterns of diversity and salt tolerance in the model halophyte seashore paspalum (Paspalum vaginatum). *Molecular Ecology*, *30*(1), 148-161. DOI: 10.1111/mec.15715

Hatfield, J. L., Reginato, R. J., & Idso, S. B. (1984). Evaluation of canopy temperature—evapotranspiration models over various crops. *Agricultural and forest meteorology*, *32*(1), 41-53. https://doi.org/10.1016/0168-1923(84)90027-3

Heimovaara, T. J., de Water, E., Dekker, S.C. (1996). A computer controlled TDR system for measuring water content and bulk electrical conductivity of soils. *Lab. of Physical Geography and Soil Science University of Amsterdam*, *41*.

Herben, T., & Hara, T. (2003). Spatial pattern formation in plant communities. In *Morphogenesis and pattern formation in biological systems* (pp. 223-235). Springer, Tokyo. https://doi.org/10.1007/978-4-431-65958-7_19

Hodges, B. P., Baldwin, C. M., Stewart, B., Tomaso-Peterson, M., McCurdy, J. D., Blythe, E. K., & Philley, H. W. (2016). Quantifying a daily light integral for establishment of warm-season cultivars on putting greens. *Crop Science*, *56*(5), 2818-2826. https://doi.org/10.2135/cropsci2015.11.0682

Hong, M., Bremer, D. J., & van der Merwe, D. (2019). Thermal imaging detects early drought stress in turfgrass utilizing small unmanned aircraft systems. *Agrosystems, Geosciences & Environment*, *2*(1), 1-9. https://doi.org/10.2134/age2019.04.0028

Huang, J., Yu, H., Guan, X., Wang, G., & Guo, R. (2016). Accelerated dryland expansion under climate change. *Nature Climate Change*, *6*(2), 166-171. https://doi.org/10.1038/nclimate2837

Ingrisch, J., & Bahn, M. (2018). Towards a comparable quantification of resilience. *Trends in Ecology & Evolution*, *33*(4), 251-259. https://doi.org/10.1016/j.tree.2018.01.013

Jespersen, D., Leclerc, M., Zhang, G., & Raymer, P. (2019). Drought performance and physiological responses of bermudagrass and seashore paspalum. *Crop Science*, *59*(2), 778-786. https://doi.org/10.2135/cropsci2018.07.0434

Jiang, Y., Duncan, R. R., & Carrow, R. N. (2004). Assessment of low light tolerance of seashore paspalum and bermudagrass. *Crop Science*, *44*(2), 587-594. https://doi.org/10.2135/cropsci2004.5870

Kéfi, S., Eppinga, M. B., de Ruiter, P. C., & Rietkerk, M. (2010). Bistability and regular spatial patterns in arid ecosystems. *Theoretical Ecology*, *3*(4), 257-269. DOI 10.1007/s12080-009-0067-z

Kéfi, S., Rietkerk, M., Alados, C. L., Pueyo, Y., Papanastasis, V. P., ElAich, A., & De Ruiter, P. C. (2007). Spatial vegetation patterns and imminent desertification in Mediterranean arid ecosystems. *Nature*, *449*(7159), 213-217. https://doi.org/10.1038/nature06111

Kopec, D. M., Walworth, J. L., Gilbert, J. J., Sower, G. M., & Pessarakli, M. (2007). 'SeaIsle 2000'paspalum putting surface response to mowing height and nitrogen fertilizer. *Agronomy journal*, *99*(1), 133-140. https://doi.org/10.2134/agronj2005.0226

Lakanmi, O. O., & Okusanya, O. T. (1990). Comparative ecological studies of Paspalum vaginatum and Paspalum orbiculare in Nigeria. *Journal of tropical ecology*, *6*(1), 103-114.

Lassu, T., Seeger, M., Peters, P., & Keesstra, S. D. (2015). The Wageningen rainfall simulator: Set-up and calibration of an indoor nozzle-type rainfall simulator for soil erosion studies. *Land Degradation & Development*, *26*(6), 604-612. https://doi.org/10.1002/ldr.2360

Legendre, P., & Fortin, M. J. (1989). Spatial pattern and ecological analysis. *Vegetatio*, *80*(2), 107-138. https://doi.org/10.1007/BF00048036

Lejeune, O., Couteron, P., & Lefever, R. (1999). Short range co-operativity competing with long range inhibition explains vegetation patterns. *Acta Oecologica*, *20*(3), 171-183. https://doi.org/10.1016/S1146-609X(99)80030-7

Martinez-Garcia, R., Cabal, C., Bonachela, J. A., Calabrese, J. M., Hernández-García, E., López, C., & Tarnita, C. E. (2021). Spatial self-organization of vegetation in water-limited systems: mechanistic causes, empirical tests, and ecosystem-level consequences. *arXiv preprint arXiv:2101.07049*.

Mayor, A. G., Bautista, S., Rodriguez, F., & Kéfi, S. (2019). Connectivity-mediated ecohydrological feedbacks and regime shifts in drylands. *Ecosystems*, *22*(7), 1497-1511. https://doi.org/10.1007/s10021-019-00366-w

Mayor, A. G., Kéfi, S., Bautista, S., Rodríguez, F., Cartení, F., & Rietkerk, M. (2013). Feedbacks between vegetation pattern and resource loss dramatically decrease ecosystem resilience and restoration potential in a simple dryland model. *Landscape ecology*, *28*(5), 931-942. https://doi.org/10.1007/s10980-013-9870-4

MEA (Millennium ecosystem assessment). (2005). *Ecosystems and human well-being* (Vol. 5). Washington, DC: Island Press.

Meron, E. (2011). Modeling dryland landscapes. *Mathematical Modelling of Natural Phenomena*, *6*(1), 163-187. https://doi.org/10.1051/mmnp/20116109

Meron, E. (2012). Pattern-formation approach to modelling spatially extended ecosystems. *Ecological Modelling*, *234*, 70-82. https://doi.org/10.1016/j.ecolmodel.2011.05.035

Meron, E., Gilad, E., von Hardenberg, J., Shachak, M., & Zarmi, Y. (2004). Vegetation patterns along a rainfall gradient. *Chaos, Solitons & Fractals*, *19*(2), 367-376. https://doi.org/10.1016/S0960-0779(03)00049-3

Ntoulas, N., & Nektarios, P. A. (2015). Paspalum vaginatum drought tolerance and recovery in adaptive extensive green roof systems. *Ecological Engineering*, *82*, 189-200. https://doi.org/10.1016/j.ecoleng.2015.04.091

Ntoulas, N., & Nektarios, P. A. (2017). Paspalum vaginatum NDVI when Grown on Shallow Green Roof Systems and under Moisture Deficit Conditions. *Crop Science*, *57*(S1), S-147. https://doi.org/10.2135/cropsci2016.05.0381

Ntoulas, N., Nektarios, P. A., Kotopoulis, G., Ilia, P., & Ttooulou, T. (2017). Quality assessment of three warm-season turfgrasses growing in different substrate depths on shallow green roof systems. *Urban Forestry & Urban Greening*, *26*, 163-168. https://doi.org/10.1016/j.ufug.2017.03.005

Pessarakli, M. (2017). Growth Responses of Sacaton Grass (Sporobolus airoides Torr.) and Seashore Paspalum (Paspalum vaginatum Swartz) Under Prolonged Drought Stress Condition. *Adv Plants Agric Res*, *7*(4), 320-326. DOI:10.15406/apar.2017.07.00261

Prăvălie, R. (2016). Drylands extent and environmental issues. A global approach. *Earth-Science Reviews*, *161*, 259-278. https://doi.org/10.1016/j.earscirev.2016.08.003

Puigdefábregas, J. (2005). The role of vegetation patterns in structuring runoff and sediment fluxes in drylands. *Earth Surface Processes and Landforms: The Journal of the British Geomorphological Research Group*, *30*(2), 133-147. https://doi.org/10.1002/esp.1181

Rahayu, R., Zuamah, H., Yang, G. M., & Choi, J. S. (2014). Growth of zoysiagrass and seashore paspalum on volcano eruption sand and clayey soil with organic and inorganic fertilizers in Indonesia. *Weed & Turfgrass Science*, *3*(3), 240-245. https://doi.org/10.5660/WTS.2014.3.3.240

Reynolds, J. F., Smith, D. M. S., Lambin, E. F., Turner, B. L., Mortimore, M., Batterbury, S. P., ... & Huber-Sannwald, E. (2007). Global desertification: building a science for dryland development. *science*, *316*(5826), 847-851. DOI: 10.1126/science.1131634

Rietkerk, M., & van de Koppel, J. (1997). Alternate stable states and threshold effects in semi-arid grazing systems. *Oikos*, 69-76. https://doi.org/10.2307/3546091

Rietkerk, M., & Van de Koppel, J. (2008). Regular pattern formation in real ecosystems. *Trends in ecology & evolution*, *23*(3), 169-175. https://doi.org/10.1016/j.tree.2007.10.013

Rietkerk, M., Boerlijst, M. C., van Langevelde, F., HilleRisLambers, R., de Koppel, J. V., Kumar, L., ... & de Roos, A. M. (2002). Self-organization of vegetation in arid ecosystems. *The American Naturalist*, *160*(4), 524-530. https://doi.org/10.1086/342078

Rietkerk, M., Dekker, S. C., De Ruiter, P. C., & van de Koppel, J. (2004). Self-organized patchiness and catastrophic shifts in ecosystems. *Science*, *305*(5692), 1926-1929. DOI: 10.1126/science.1101867

Russell, T. R., Karcher, D. E., & Richardson, M. D. (2020). Daily light integral requirements of warm-season turfgrasses for golf course fairways and investigating in situ evaluation methodology. *Crop Science*. https://doi.org/10.1002/csc2.20234

Saco, P. M., Moreno-de las Heras, M., Keesstra, S., Baartman, J., Yetemen, O., & Rodríguez, J. F. (2018). Vegetation and soil degradation in drylands: nonlinear feedbacks and early warning signals. *Current Opinion in Environmental Science & Health*, *5*, 67-72. https://doi.org/10.1016/j.coesh.2018.06.001

Scheffer, M., Bascompte, J., Brock, W. A., Brovkin, V., Carpenter, S. R., Dakos, V., ... & Sugihara, G. (2009). Early-warning signals for critical transitions. *Nature*, *461*(7260), 53-59. https://doi.org/10.1038/nature08227

Scheffer, M., Carpenter, S. R., Dakos, V., & van Nes, E. H. (2015). Generic indicators of ecological resilience: inferring the chance of a critical transition. *Annual Review of Ecology, Evolution, and Systematics*, *46*, 145-167. https://doi.org/10.1146/annurev-ecolsys-112414-054242

Scheffer, M., Carpenter, S., Foley, J. A., Folke, C., & Walker, B. (2001). Catastrophic shifts in ecosystems. *Nature*, *413*(6856), 591-596. https://doi.org/10.1038/35098000

Schneider, F. D., & Kéfi, S. (2016). Spatially heterogeneous pressure raises risk of catastrophic shifts. *Theoretical Ecology*, *9*(2), 207-217. https://doi.org/10.1007/s12080-015-0289-1

Thompson, S. E., & Daniels, K. E. (2010). A porous convection model for grass patterns. *The American Naturalist*, *175*(1), E10-E15. https://doi.org/10.1086/648603

Thompson, S., Katul, G., & McMahon, S. M. (2008). Role of biomass spread in vegetation pattern formation within arid ecosystems. *Water Resources Research*, *44*(10). https://doi.org/10.1029/2008WR006916

USGA Recommendations for a Method of Putting Green Construction, 2004. https://www.usga.org/content/dam/usga/images/course-care/2004%20USGA%20Recommendations%20For%20a%20Method%20of%20Putting%20Green%20Cons.pdf

Vincenot, C. E., Carteni, F., Mazzoleni, S., Rietkerk, M., & Giannino, F. (2016). Spatial self-organization of vegetation subject to climatic stress—insights from a system dynamics—individual-based hybrid model. *Frontiers in plant science*, *7*, 636. https://doi.org/10.3389/fpls.2016.00636

von Hardenberg, J., Meron, E., Shachak, M., & Zarmi, Y. (2001). Diversity of vegetation patterns and desertification. *Physical Review Letters*, *87*(19), 198101. https://doi.org/10.1103/PhysRevLett.87.198101

Wang, X., Cammeraat, E. L., Romeijn, P., & Kalbitz, K. (2014). Soil organic carbon redistribution by water erosion–the role of CO 2 emissions for the carbon budget. *PLoS One*, *9*(5), e96299. https://doi.org/10.1371/journal.pone.0096299

Zhang, J., Glenn, B., Unruh, J. B., Kruse, J., Kenworthy, K., Erickson, J., ... & Trenholm, L. (2017). Comparative Performance and Daily Light Integral Requirements of Warm-Season Turfgrasses in Different Seasons. *Crop Science*, *57*(4), 2273-2282. https://doi.org/10.2135/cropsci2017.01.0052

Zhou, Y., Lambrides, C. J., Kearns, R., Ye, C., & Fukai, S. (2012). Water use, water use efficiency and drought resistance among warm-season turfgrasses in shallow soil profiles. *Functional plant biology*, *39*(2), 116-125. https://doi.org/10.1071/FP11244

Appendix A: NDVI measurements

Next to the results presented from the thermal and normal camera, also pictures to determine NDVI were taken. To capture the part of the spectrum needed for NDVI, a Sony α6000 camera (24.3 mp) was converted (using a Kolari Blue IR NDVI 49 mm Pro slim lens) into capturing only Blue(B), and Near Infrared (NIR). Although pictures with this camera were taken on a regular basis during the experiment, they were decided not to include as results. In most circumstances NDVI is measured outside, where there is direct sunlight. In the lab all light coming from outside was blocked, leaving only the light from the grow lights to ensure homogenous illumination of the grass. With the limited emission spectrum of the grow lights, e.g. no NIR emission, NDVI cannot be determined. To compensate a halogen light with a broad emission spectrum was installed. However, a homogenous illumination of the entire grass surface turned out to be too challenging. Figure 6 presents two clipped parts of unprocessed NDVI pictures. For these the picture the illumination was decent, but overall the quality of the pictures was deemed not sufficient for further analysis.

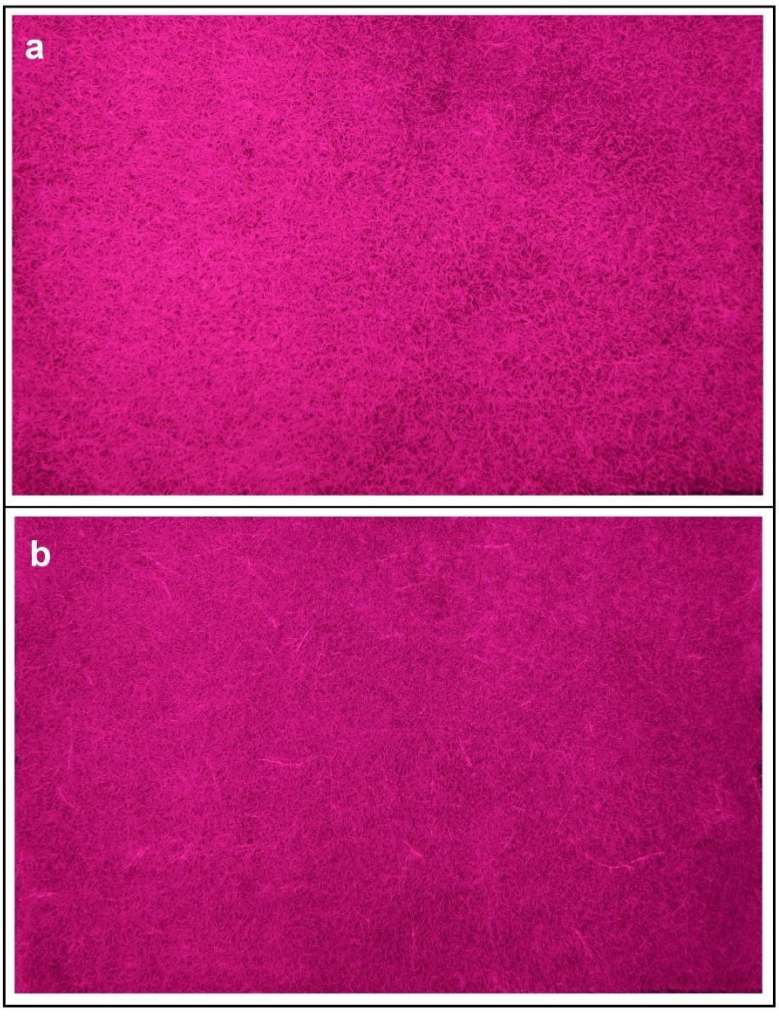

Figure 7 | Unprocessed NDVI footage. Lighter colors indicate more active reflection of NIR, corresponding to better plant health. Although these picture are not processed and therefore not accurately indicate NDVI values, the difference in color already show some differences in plant health. **a)** Right half of the 25% ET treatment plot on day 9. **b)** Right half of the 25% ET treatment plot on day 31. Note the overall loss of plant health of b compared to a, but also the increase of (active) explorative rhizomes and ramet, related to the foraging behavior of clonal reproduction.

Appendix B: Reference green cover

Figure 8 | Reference green cover. Picture of the *P.vaginatum* grass cover 3 days before the start of the experiment.

Appendix C: Air temperature anomaly

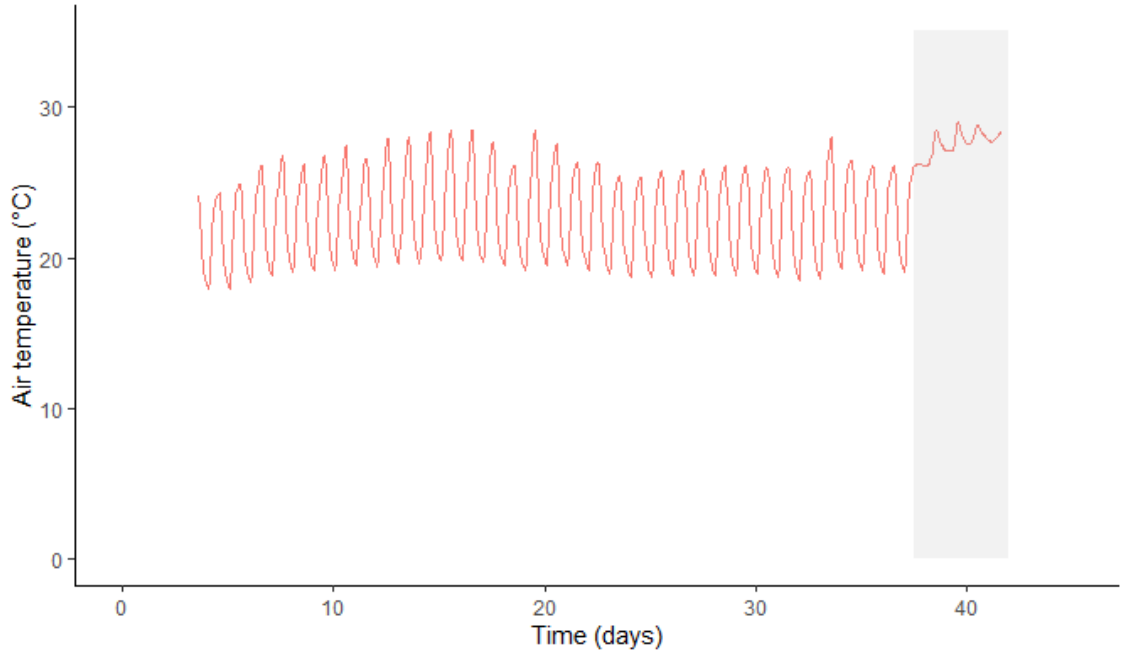

Figure 9 | Average air temperature. The average air temperature, measured at the middle of the left and right sight of the flume on a height of approximately one meter from the canopy. The air temperature fluctuates between a minimum at night and a maximum during the day. The grey shade indicates the change in air circulation in the last week, causing an higher average temperature.